

Supporting Information

Solution-Processed CdS/Cu₂S Superlattice Nanowire with Enhanced Thermoelectric Property

Ze Xiong,^{†,§} Yu Cai,^{†,§} Xiaodong Ren,[‡] Bei Cao,^{†,||} Jianjun Liu[#], Ziyang Huo,^{⊥,*} and
Jinyao Tang^{†*}

[†]Department of Chemistry, The University of Hong Kong, Hong Kong 999077, China.

[‡]State Key Laboratory of Functional Materials for Informatics, Shanghai Institute of Microsystem and Information Technology, Chinese Academy of Sciences, Shanghai 200050, China

^{||}State Key Laboratory of Synthetic Chemistry, The University of Hong Kong, Hong Kong 999077, China

[#]State Key Laboratory of High Performance Ceramics and Super fine Microstructures, Shanghai Institute of Ceramics, Chinese Academy of Sciences, Shanghai 200050, China

[⊥]Queensland Micro- and Nanotechnology Center, Nathan Campus, Griffith University, Brisbane 4111, Australia

Corresponding Author

Z.H.(ziyanghuo@gmail.com) and J.T. (jinyao@hku.hk).

Sample preparation:

Physical vapor deposition (PVD) growth of CdS nanowire

To grow CdS nanowires, 10 nm gold was deposited on the surface of a silicon wafer by thermal evaporation at a deposition rate of 0.5 Å/s. Crucible filled with CdS powders (99.9 %, Aldrich) was loaded into a one inch quartz tube as the CdS source. The Si wafer with gold was placed at downstream position of the CdS source. Ar as a carrier gas was introduced at a flow rate of 100 sccm during the whole growing process. The temperature was ramped up to 780 °C (in 10 min) and kept stable for 30 min. The wafer was taken out after the furnace was cooled down to the room temperature. The diameters of the CdS nanowires lie in the range of 80 - 200 nm and their length can reach ~ 100 μm.

Cation exchange reaction in the CdS nanowires

A modified approach was adopted based on the cation exchange reaction to form CdS/Cu₂S core-shell solar cell reported recently:¹ silicon wafer of 0.5 cm × 0.5 cm was washed by deionized water, acetone and IPA, then cleaned by oxygen plasma at the oxygen flow rate of 10 sccm for 30 s to make the surface hydrophilic. 0.16 g CuCl was dissolved in the 15 ml N₂H₄/HCl solution (pH ≈ 7), which was heated to 80 °C for 1h to fully dissolve the CuCl powder. A cleaned Si wafer with CdS nanowires scraped from the as-growth wafer was immersed in the CuCl solution for the ion exchange reaction. After specified reaction time, the wafer was taken out of the solution immediately, washed by deionized water and gently blown dry by compressed nitrogen.

Solution-liquid-solid (SLS) growth of Cu₂S nanowire

CuCl₂ powder and Na(I)[S₂CNC₄H₁₀] were separately dissolved in deionized water and then mixed in the mole ratio of more than 2:1 (ligand to metal) to form Cu precursor particles.² A piece of silicon wafer was immersed in 5:1 BHF for 1 min to get rid of the oxidation layer on the surface, then washed by water and IPA and carefully dried with compressed nitrogen gas. Then 10 nm bismuth was deposited on the on a piece of silicon wafer by thermal evaporation at the deposition rate of 0.5 Å/s as the catalyst for the solution-liquid-solid (SLS) growth of Cu₂S nanowires. The Si wafer with bismuth was then cut into 0.2 cm × 0.5 cm chips for further growth process. 0.1 g Cu precursor particles were dissolved in 1 mL trioctylphosphine (97%, Aldrich) in a glass tube which was sealed by butane gas flame after loading the silicon wafer. Then the glass tube was heated in a sand bath at 300 °C for 20 min in a muffle furnace to obtain a large amount of Cu₂S nanowires. After the reaction, the solution was dispersed in 30 mL toluene and centrifuged at 3000 rpm for 10 minutes for 3 times. The Cu₂S nanowires after centrifugation was dispersed in IPA and dropped onto the oxidized Si wafer for device fabrication. From the SEM characterization, it can be found that the length of the Cu₂S nanowires can reach ~ 40 μm and the diameters was in the range of 100 to 200 nm.

Device Fabrication

To avoid the PMMA residue during e-beam lithography and get a good contact between electrodes and the synthesized nanowire, 10 nm Al₂O₃ layer was deposited with atomic layer deposition (ALD) at 70 °C using trimethylaluminum (98 %,

Aldrich). Then 3 wt.% diphenylsilanediol (DPSD, Aldrich) in ethanol was spin-coated on the surface of the wafer at 4000 rpm/s for 40s and baked on a hotplate at 120 °C for 5 min to promote the adhesion of PMMA to the wafer surface. 8 wt.% Poly(methyl methacrylate) (PMMA) in anisole was spin-coated on the surface of the wafer at 4000 rpm/s for 40s to form a 1 μ m PMMA layer and baked on a hotplate at 120 °C for 45 min to ensure that the PMMA was well adhered to the wafer surface. After e-beam lithography and development. The device was dipped into 5:1 BHF (40% NH_4F : 49% HF , v/v, 5:1) for 5 s to remove the Al_2O_3 over the electrode area. Immediately after the wet etching, 10 nm Cr/300 nm Ni/10 nm Au was deposited by thermal evaporator and lifted off in 10 % CH_2Cl_2 + 90 % acetone.

Characterizations:

Powder X-ray diffraction (XRD) patterns of synthesized nanowires were recorded using Bruker D8 ADVANCE X-ray diffractometer with $\text{Cu K}\alpha$ radiation ($\lambda = 1.5418$ Å). The transmission electron microscopy (TEM) and high-resolution TEM (HRTEM) images were taken with a FEI Tecnai TEM. The scanning electron microscopy (SEM) images were taken with a Hitachi S4800 FEG SEM.

Modeling details:

The interface formation energy, involving surface energy and separation work are calculated for each interface. The thicknesses of vacuum slab for all the interface models were 10 Å. The structural relaxation (Table S1) and interface formation energies calculations were performed by using VASP code³ with the

projector-augmented wave (PAW) potentials.⁴ Generalized gradient (GGA) corrections were applied to the exchange-correlation function within the implementation of Perdew, Burke, and Ernzerhof (PBE).⁵ After the full convergence test, the kinetic energy cutoff of the plane wave basis was chosen to be 250 eV. The Brillouin zone of supercell are sampled in the k-space within the Monkhorst–Pack scheme⁶ for the self-consistent structure optimizations and the total energy calculations, respectively. The mesh points are selected according to the size of the cell. For interface models, Γ point K-mesh were used. All atomic positions and lattice parameters are optimized by using the conjugate gradient method where total energy and atomic forces are minimized. The convergence for energy is chosen as 10^{-4} eV between two ionic steps, and the maximum force allowed on each atom is 0.01 eV/Å.

Thermoelectric measurement:

To detect the temperature gradient (ΔT) over the nanowire, the temperature coefficient of resistance (TCR) of the two thermometers was first obtained by four probe measurement at different environment temperatures. After the calibration of the thermometers, a heating current was applied to the heater and the resistance of thermometers were measured at the same time. The ΔT can be calculated by $\Delta T = \Delta T_{\text{hot}} - \Delta T_{\text{cold}}$. Figure S7 shows the details of our measurement setup. A Keithley 236 source meter was used as the DC source to apply the heating current and measure the electrical conductivity. Two Lock-in amplifiers SR810 were used for the thermometer resistance measurement. In addition, a Keithley 2182 nanovoltmeter was used for the thermopower measurement. All the measurements were performed in a cryostat with

high vacuum. The diameters of the CdS nanowires lie in the range of and their length can reach $\sim 100 \mu\text{m}$.

The error analysis follows the protocol adopted in our previous work.⁷ The nanowires are usually 80 - 200 nm in width and $\sim 1.5 \mu\text{m}$ in length between the two thermometers. Most uncertainty of σ measurement is coming from the wire diameter measurement which can vary up to 3.5% across different samples. Since the uncertainty from electrical measurement noise is less than 0.1%, we regard the uncertainty of σ measurement as 3.5% as the linear regression method error estimated by the software (origin). For the thermopower measurement, the uncertainty of this measurement is estimated as less than 4% due to possible systematic errors of this method. The error of power factor (11.5 %) is obtained by considering the propagation of error.

Table S1. Comparison of experimental lattice parameters⁸⁻⁹ to relaxed lattice parameters for CdS and Cu₂S crystals obtained within GGA.

Lattice	Space group	a (Å)		b (Å)		c (Å)	
		Relaxed	Exp.	Relaxed.	Exp.	Relaxed	Exp.
Cu ₂ S	P21/c (14)	15.164	15.246	11.914	11.884	13.372	13.494
CdS	P63mc (186)	4.199	4.136	4.199	4.136	6.818	6.716

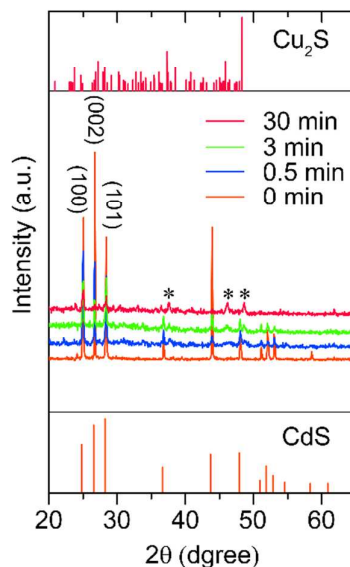


Figure S1. XRD patterns of pristine CdS nanowires and partially converted CdS/Cu₂S nanowires formed with increasing cation exchange reaction time (from bottom to top, 0 min, 0.5 min, 3 min and 30 min). The prolonged reaction time leads to gradual conversion of the wurtzite nanowires into the low-temperature phase of chalcocite Cu₂S (L-Cu₂S). The major peaks corresponding the Cu₂S are denoted by asterisk (*). Patterns from the Joint Committee on Powder Diffraction Standards (JCPDS) for wurtzite CdS (bottom yellow, JCPDS no. 00-041-1049, space group P6₃mc (No. 186)) and low-temperature chalcocite Cu₂S (top red, JCPDS no. 00-033-0490, space group P2₁/c (No. 14)) are included for reference.

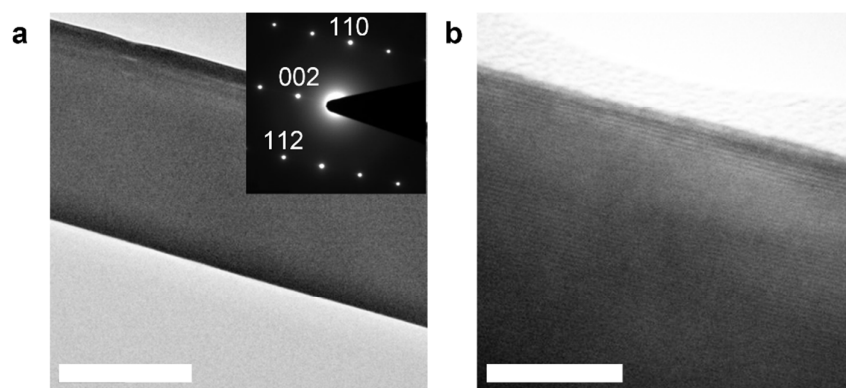


Figure S2. (a) TEM and (b) HRTEM images of pristine CdS nanowire, showing a preferential nanowire growth along $\langle 0002 \rangle$ direction. Inset: electron diffraction pattern taken on the single crystalline nanowire. Scale bars: (a) 200 nm; (b) 10 nm.

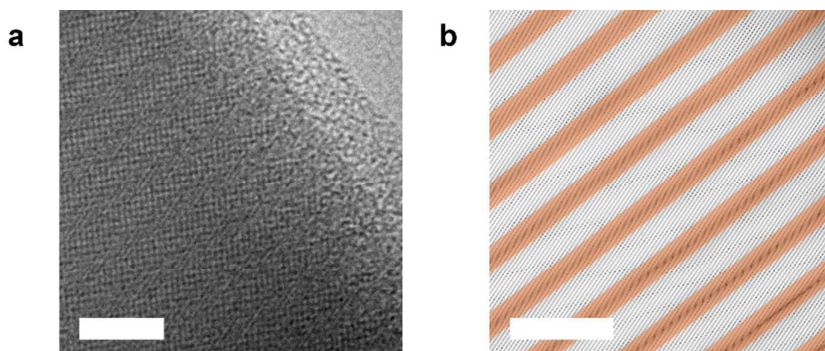


Figure S3. (a) High-resolution TEM image of a CdS/Cu₂S superlattice nanowire. (b) Constructed inverse FFT image of (a). The orange and white color is used to clarify the superlattice structure. Scale bar: 5 nm.

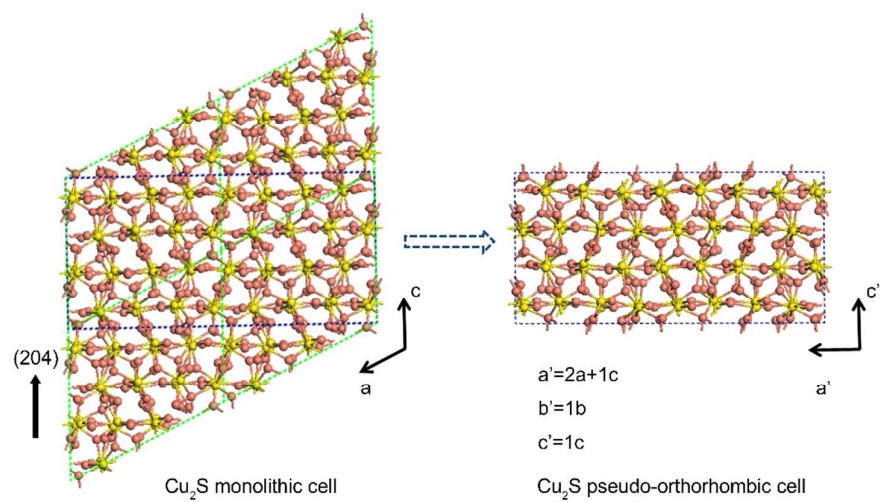


Figure S4. Relationship between the monoclinic unit cell (denoted by green dashed line) of low temperature chalcocite Cu_2S and the pseudo-orthorhombic cell (denoted by blue dashed line).

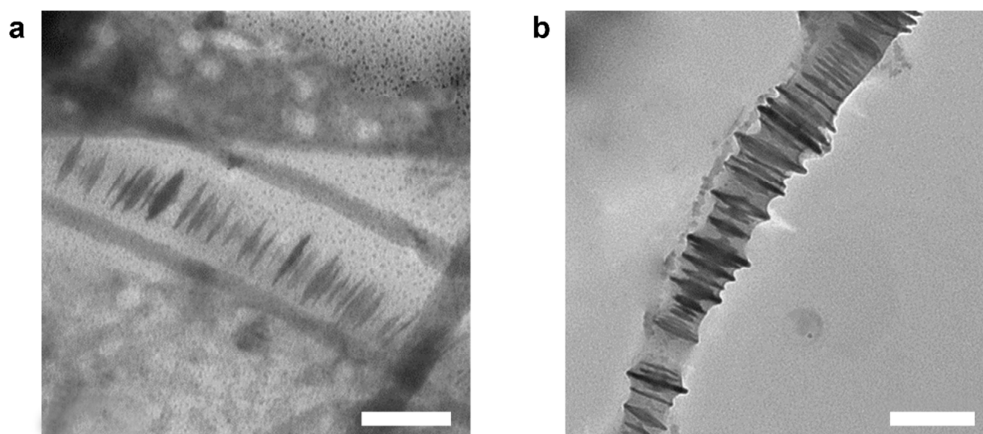


Figure S5. TEM images of CdS/Cu₂S superlattice nanowire (a) with and (b) without remained Cu₂S shell after removal of CdS by 0.1 M HCl. Scale bars: 100 nm.

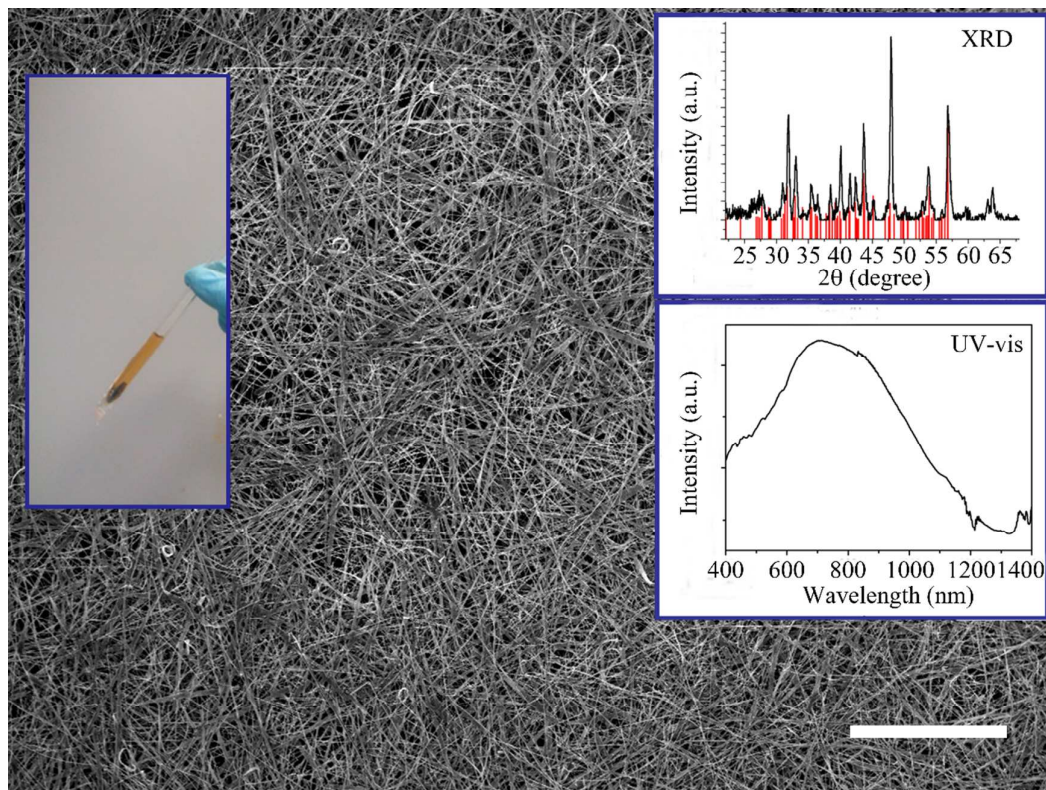


Figure S6. The SEM image of as synthesized Cu₂S nanowires. Scale bar: 30 μm. Insets: (left) optical image of synthesized Cu₂S nanowires; (upper right) XRD pattern of Cu₂S nanowires with low-temperature chalcocite Cu₂S pattern for reference (JCPDS no. 00-033-0490, space group P21/c (No. 14)); (bottom right) absorbance of Cu₂S nanowires.

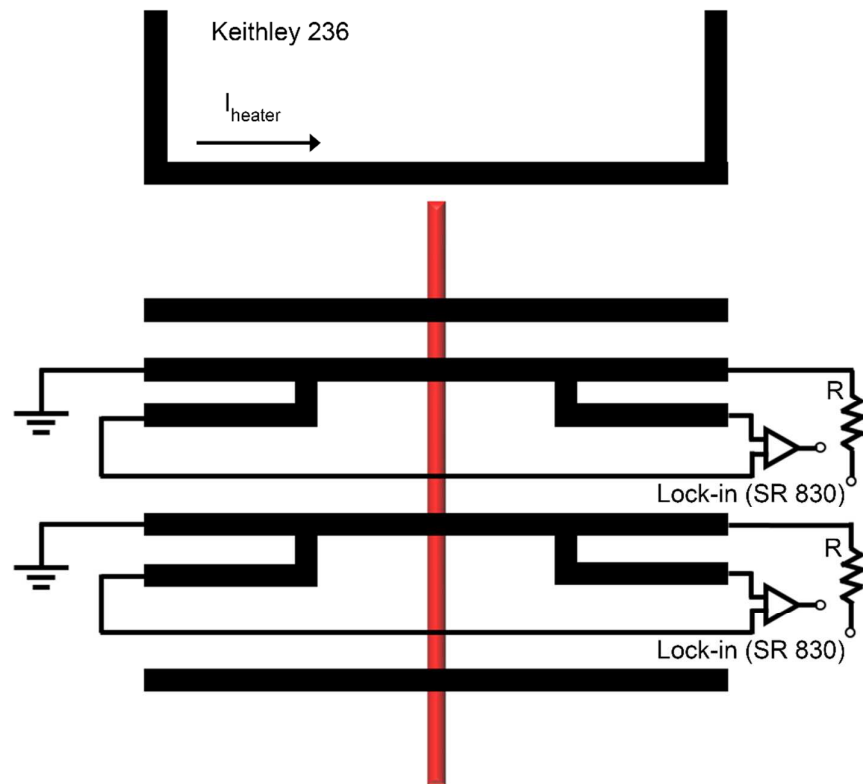


Figure S7. The thermoelectric measurement setup.

References

1. Tang, J. Y.; Huo, Z. Y.; Brittman, S.; Gao, H. W.; Yang, P. D., Solution-Processed Core-Shell Nanowires for Efficient Photovoltaic Cells. *Nat. Nano.* **2011**, *6* (9), 568-572.
2. Jen-La Plante, I.; Zeid, T. W.; Yang, P.; Mokari, T., Synthesis of Metal Sulfide Nanomaterials Via Thermal Decomposition of Single-Source Precursors. *J. Mater. Chem.* **2010**, *20* (32), 6612-6617.
3. Kresse, G.; Furthmüller, J., Efficient Iterative Schemes for Ab Initio Total-Energy Calculations Using a Plane-Wave Basis Set. *Phy. Rev. B.* **1996**, *54* (16), 11169-11186.
4. Blöchl, P. E., Projector Augmented-Wave Method. *Phy. Rev. B.* **1994**, *50* (24), 17953-17979.
5. Perdew, J. P.; Burke, K.; Ernzerhof, M., Generalized Gradient Approximation Made Simple. *Phys. Rev. Lett.* **1996**, *77* (18), 3865-3868.
6. Monkhorst, H. J.; Pack, J. D., Special Points for Brillouin-Zone Integrations. *Phy. Rev. B.* **1976**, *13* (12), 5188-5192.
7. Tang, J. Y.; Wang, H. T.; Lee, D. H.; Fardy, M.; Huo, Z. Y.; Russell, T. P.; Yang, P. D., Holey Silicon as an Efficient Thermoelectric Material. *Nano. Lett.* **2010**, *10* (10), 4279-4283.
8. Cook, W. R.; Shiozawa, L.; Augustine, F., Relationship of Copper Sulfide and Cadmium Sulfide Phases. *J. Appl. Phys.* **1970**, *41* (7), 3058-3063.
9. Evans, H. T., Crystal Structure of Low Chalcocite. *Nat. Phys. Sci.* **1971**, *232*, 69-70.